Quantum-Admixture Model of High-Spin ↔ Low-Spin Transition for Fe(III) Complex Molecules†

Kuang Xiao-Yu*

Institute of Atomic and Molecular Physics, Sichuan University, Chengdu 610065, China; International Centre for Materials Physics, Academia Sinica, Shenyang 110015, China

Zhou Kang-Wei

Department of Physics, Sichuan University, Chengdu 610064, China; CCAST (World Laboratory), Box 8730, Beijing 100080; International Centre for Materials Physics, Academia Sinica, Shenyang 110015, China

Received: August 12, 1999; In Final Form: November 19, 1999

A quantum admixture model for the d^5 configuration of the high-spin ↔ low-spin (HS ↔ LS) transition ($^6A_1 \leftrightarrow {}^2T_2$) Fe(III) complex molecules has been established by using the UCFC scheme. The analysis shows that there exists an indirect spin−orbital coupling interaction between the high-spin and low-spin states via the intermediate-spin states. This interaction may be described approximately by two small matrices (the order is 25 and 14, respectively) of the Hamiltonian, which involves the electron−electron repulsion, the ligand-field, the spin−orbit coupling, and the Zeeman interactions. By diagonalizing these matrices, the electronic and magnetic structures of the Fe(III) molecules in the spin-transition region can be derived. The results show a sensitive dependence on the ratio $\Delta Dq/\zeta$. Here ζ is the spin−orbit coupling coefficient and $\Delta Dq = Dq - Dq_0$, while Dq_0 is the ligand-field strength at the spin-transition point. From this model a reasonable explanation for the temperature-dependent magnetic moment of the Fe(III) in $[Fe(3-OEt-SalAPA)_2]ClO_4 \cdot C_6H_6$ molecules has been given.

I. Introduction

The high-spin ↔ low-spin (HS ↔ LS) transition ($^6A_1 \leftrightarrow {}^2T_2$) of a Fe(III) complex molecule is such a course that the ground state of the Fe(III) ion changes from a high-spin state $^6A_1$ (a state whose whole or major component is of high spin) into a low-spin state $^2T_2$ (a state whose whole or major component is of low spin) when the value of the crystal field strength parameter Dq changes over a small region, which may be called spin-transition region. A spin transition may be looked upon as a discontinuous type only if the spin-transition region is very small.

The magnetic properties of a Fe(III) molecule in the HS ↔ LS transition region are very different from those in the typical high-spin state $^6A_1$ or in the low-spin state $^2T_2$. For example, the magnetic moment may vary unusually from 5.9 μ_B to 2.0 μ_B. The interesting spin-transition phenomena had been widely studied experimentally and theoretically[1−14] and had been attributed to an intra-ionic transfer with a spin flip of the transferred electrons. In order to study the temperature dependence of the magnetic moment, a thermal spin-equilibrium model[1] and some quantum-mechanical-mixture models[10−14] have been proposed and some progresses have been made. However, due to the limitation of the weak-field scheme used in the previous quantum-mechanical-mixture models, up to now, the physical mechanism and the main interactions that govern the HS ↔ LS transition have not yet been determined. As for in refs 10 and 11, the problems treated are only $^6A_1 \leftrightarrow {}^4A_1$ spin-transition ones.

In order to study the HS ↔ LS transitions mentioned above, we will suggest a new quantum-admixture model based on the unified-crystal-field-coupling (UCFC) scheme.[16] The UCFC scheme is neither a weak-field scheme nor a usual strong-field scheme, although it uses a special strong-field representation.[15] It has a complete matrix (the order is 252) of the interaction Hamiltonian, involving electron−electron repulsion H_{ee}, ligand-field H_c, spin−orbit coupling H_{so}, and Zeeman interactions H_M.

It is shown from our theoretical analysis by using the UCFC scheme that there exists between the states $^6A_1$ and $^2T_2$ an indirect spin−orbit coupling interaction, which is caused by the intermediate spin state $^4T_1$ and is mainly responsible for this HS ↔ LS transition. This important coupling way may be written as $^6A_1-{}^4T_1-{}^2T_2$, and this coupling model may be described by four much smaller matrices, which are obtained by a simplification from the complete matrix in the UCFC method.[16] The results calculated from the small matrices are very close to those from the complete matrix.

The four small matrices mentioned above will be introduced with detail in section II. A general study for the electronic structure and the magnetic properties of HS ↔ LS transition Fe(III) molecules will be given in section III. An explanation about the temperature dependence of the magnetic moment of the Fe(III) in $[Fe(3-OEt-SaLAPA)_2]ClO_4 \cdot C_6H_6$ molecules will be given in section IV.

II. The Interaction Matrix and the $^6A_1-{}^4T_1-{}^2T_2$ Coupling Model

The complete matrix of the interaction Hamiltonian that involves only $H_{ee} + H_c + H_{so}$ of a cubic d^5 ion has been established by Zhou et al.[15] in the spin−orbit coupling repre-

† This project was supported by National Natural Science Foundation of China.

10.1021/jp992864g CCC: $19.00
Published on Web 07/18/2000

TABLE 1: Elements of the Upper Triangle Part of the Symmetric Matrix $\mathbf{M}_1'$ (14 × 14)

$E'\alpha'$	$U'\lambda$			
$^4T_1$	$^6A_1$	$^4T_1$	$^4T_1'$	$^2T_2(10)$
$-25B + 6C$ $-10Dq + 5\zeta/12$ $-(^1/_6 - 5g/6)\,H$	0	$-H(^1/_6 - g/3)\sqrt{5}$	$gH(1/3)\sqrt{5}$	0
	$-35B + (^1/_2)\,gH$	0	$-\zeta\sqrt{2}$	0
		$-25B + 6C$ $-10Dq + \zeta/6 + (^1/_{15} + 11g/30)\,H$	$-(^3/_{10} - 3g/5)\,H$	$\mathbf{Z}'$
			$-25B + 6C$ $-10Dq - \zeta/4 + (^1/_{10} + 3g/10)\,H$	$-2\,\mathbf{Z}'$ $\mathbf{V} + \mathbf{Z}$ $(\mathbf{L} - g\mathbf{E}/2)\,H$

TABLE 2: Elements of the Upper Triangle Part of the Symmetric Matrix $\mathbf{M}_3'$ (25 × 25)

$E''\alpha''$			$U'\nu$			
$^6A_1$	$^4T_1$	$^2T_2$ (10)	$^6A_1$	$^4T_1$	$^4T_1$	$^2T_2$ (10)
$-35B$ $-(^5/_6)\,gH$	$-\zeta\sqrt{2}$	0	$gH(2/3)\sqrt{5}$	0	0	0
	$-25B + 6C$ $-10Dq - \zeta/4$ $-(^1/_6 + g/2)H$	$\mathbf{Z}'\sqrt{10}$	0	$H(^1/_{10} - g/5)\sqrt{5}$	$H(^1/_{15} + g/5)2\sqrt{5}$	0
		$\mathbf{V} - 2\mathbf{Z}$ $-(2\mathbf{L}/3 + g\mathbf{E}/6)\,H$	0	0	0	$-H(\mathbf{L}/3 + g\mathbf{E}/3)\sqrt{2}$
			$-35B$ $+(^{11}/_6)\,gH$	0	$-\zeta\sqrt{2}$	0
				$-25B + 6C$ $-10Dq + \zeta/6$ $-(^1/_5 + 11g/10)\,H$	$-(^1/_{10} - g/5)\,H$	$\mathbf{Z}'$
					$-25B + 6C$ $-10Dq - \zeta/4$ $+(^{11}/_{30} + 11g/10)\,H$	$-2\,\mathbf{Z}'$ $\mathbf{V} + \mathbf{Z}$ $-(\mathbf{L}/3 - g\mathbf{E}/6)\,H$

sentation $S\Gamma\,\beta\Gamma'\gamma'$ with a standard basis that is always used in the UCFC method.[15,16] This big matrix may be reduced into eight small matrices;[15] those may be denoted respectively as

$$\begin{aligned} E'\gamma'\ (20 \times 20) \qquad & \gamma' = \alpha', \beta' \\ E''\gamma'\ (22 \times 22) \qquad & \gamma' = \alpha'', \beta'' \\ U'\gamma'\ (42 \times 42) \qquad & \gamma' = \kappa, \lambda, \mu, \nu \end{aligned} \tag{1}$$

Each of them, since its basis functions $|i, S\Gamma\,\beta\Gamma'\gamma'\rangle$ are grouped and queued according to cubic terms $S\Gamma$, is a block matrix constructed by $S\Gamma$ blocks.

Now, considering an applied magnetic field H along the z-axis, the Zeeman interaction $H_M = \mu_B\,(L_z + g_e S_Z)H$ should be introduced in the Hamiltonian, where $g_e = 2.0023$. In this case, the $\Gamma'\gamma'$ terms are coupled to one another by then Zeeman effect and then led to four matrices as follows (the number in parentheses represents the order of the matrix or the block):

$$\mathbf{M}_1(62) = \begin{bmatrix} E'\alpha'(20) & H_M \text{ elements} \\ H_M \text{ elements} & U'\lambda(42) \end{bmatrix} \qquad \mathbf{M}_2(62) = \begin{bmatrix} E'\beta'(20) & H_M \text{ elements} \\ H_M \text{ elements} & U'\mu(42) \end{bmatrix}$$

$$\mathbf{M}_3(64) = \begin{bmatrix} E''\alpha''(22) & H_M \text{ elements} \\ H_M \text{ elements} & U'\nu(42) \end{bmatrix} \qquad \mathbf{M}_4(64) = \begin{bmatrix} E''\beta''(22) & H_M \text{ elements} \\ H_M \text{ elements} & U'\mu(42) \end{bmatrix} \tag{2}$$

When $H = 0$, the diagonal $\Gamma'\gamma'$ blocks are just the matrices in (1); this leads to $\mathbf{M}_1 = \mathbf{M}_2$ and $\mathbf{M}_3 = \mathbf{M}_4$. When $H \neq 0$, Zeeman elements may occur in all diagonal and off-diagonal blocks, leading to $\mathbf{M}_1 \neq \mathbf{M}_2$ and $\mathbf{M}_3 \neq \mathbf{M}_4$.

Each of the matrices in (2) is still constructed by $S\Gamma$ blocks. This makes it very convenient to analyze the influences of the quantum states having various spin or group symmetry on the calculated spectral and magnetic results and especially convenient to study spin-transition phenomena.

In order to reveal the major mechanism of the HS ↔ LS transition and to establish a simple physical model, we have analyzed the spin−orbit interactions among the different strong-field terms $S\Gamma$ in each $\Gamma'\gamma'$ term. It is well-known, that the spin−orbit coupling should obey the selection rule $\Delta S = 0, \pm 1$. Obviously, no direct interaction can occur between the high-spin ($S = ^5/_2$) and the low-spin ($S = ^1/_2$) states. However, it is shown from our analysis that there exists an indirect coupling $^6A_1 - ^4T_1 - ^2T_2$, which is mainly responsible for this transition. Then, by taking in use only the relevant terms $^6A_1(t_2^3\,e^2)$, $^4T_1(t_2^4\,e^1)$ and $^2T_2$ (taking all the 10 configurations of $^2T_2$), the matrices in (2) can be simplified into four much smaller ones and denoted respectively as

$$\begin{aligned} &\mathbf{M}_1'\ (14 \times 14), \qquad \mathbf{M}_2'\ (14 \times 14), \\ &\mathbf{M}_3'\ (25 \times 25), \qquad \mathbf{M}_4'\ (25 \times 25) \end{aligned} \tag{3}$$

Where $\mathbf{M}_1'$ and $\mathbf{M}_3'$ are given respectively in Tables 1 and 2, and they will change respectively into $\mathbf{M}_2'$ and $\mathbf{M}_4'$ when each diagonal Zeeman element is multiplied by (−1). The notation $\mathbf{E}$ in Tables 1 and 2 express a 10 × 10 unit numerical matrix. While $\mathbf{Z}$ is the 10 × 10 matrix of the spin−orbit interaction H_{so} in the $^2T_2$ term, $\mathbf{Z}'$ is the 1 × 10 matrix of H_{so} between the terms $^4T_1$ and $^2T_2$, $\mathbf{L}$ is the 10 × 10 matrix of the operator L_z in the $^2T_2$ term, $\mathbf{V}$ is just the matrix of $(H_{ee} + H_c)$ in the $^2T_2$ term given by Griffith.[17] The upper-triangle matrix elements of $\mathbf{V}$ are listed in Table 3, while the nonzero upper-triangle matrix elements of $\mathbf{Z}$, $\mathbf{Z}'$, and $\mathbf{L}$ are listed in Table 4.

TABLE 3: Upper Triangle Part of the Symmetric Matrix V (10 × 10)

$-20Dq - 20B + 10C$	$-3B\sqrt{6}$	0	$2B\sqrt{3}$	$4B + 2C$	$2B$	0	0	0	
	$-10Dq - 8B + 9C$	$-(1/2)B\sqrt{6}$	$-(3/2)B\sqrt{2}$	$-(3/2)B\sqrt{6}$	$-(3/2)B\sqrt{6}$	0	$-(4B + C)$	0	
		$-10Dq - 18B + 9C$	$(3/2)B\sqrt{2}$	$(5/2)B\sqrt{6}$	$-(5/2)B\sqrt{6}$	$-C$	0	0	
			$-16B + 8C$	$-2B\sqrt{3}$	0	$(3/2)B\sqrt{6}$	$-(1/2)B\sqrt{6}$	0	
				$-12B + 8C$	$10B\sqrt{3}$	0	$(3/2)B\sqrt{2}$	$2B\sqrt{3}$	
					$2B + 12C$	0	$-(5/2)B\sqrt{6}$	$4B + 2C$	
						$-6B + 10C$	$(5/2)B\sqrt{6}$	$-2B$	
							$10Dq - 18B + 9C$	$B\sqrt{6}$	
								$10Dq - 8B + 9C$	$-3B\sqrt{6}$
									$20Dq - 20B + 10C$

TABLE 4: Nonzero Elements of the Matrix Z′ (1 × 10) and Those of the Upper Triangle Part of the Symmetric Matrices Z (10 × 10) and L (10 × 10) in M'_{1-4}, where Z′ refers to $\langle {}^4T_1|H_{so}|{}^2T_2\rangle$, Z refer to $\langle {}^2T_2|H_{so}|{}^2T_2\rangle$, and L refer to $\langle {}^2T_2|L_z|{}^2T_2\rangle$

Z_{ij} (in unit ζ)	Z'_{ij} (in unit ζ)	L_{ij}
$Z(1,1) = 1/2$	$Z'(1,1) = -\sqrt{30}/10$	$L(1,1) = 1$
$Z(1,2) = \sqrt{6}/12$	$Z'(1,2) = -\sqrt{5}/20$	$L(1,2) = \sqrt{6}/2$
$Z(1,3) = -\sqrt{6}/4$	$Z'(1,3) = \sqrt{5}/20$	$L(1,3) = \sqrt{6}/2$
$Z(2,2) = -1/6$	$Z'(1,4) = -\sqrt{30}/60$	$L(2,2) = -1/2$
$Z(2,3) = 1/4$	$Z'(1,5) = \sqrt{10}/10$	$L(2,4) = -\sqrt{6}/4$
$Z(2,4) = 5\sqrt{6}/24$	$Z'(1,6) = -\sqrt{30}/20$	$L(2,6) = -\sqrt{6}/4$
$Z(2,6) = \sqrt{6}/24$		$L(2,7) = \sqrt{6}/2$
$Z(2,7) = -\sqrt{6}/12$		$L(3,3) = 1/2$
$Z(3,4) = \sqrt{6}/24$		$L(3,4) = -\sqrt{6}/4$
$Z(3,5) = \sqrt{2}/4$		$L(3,5) = \sqrt{2}/2$
$Z(3,6) = -\sqrt{6}/8$		$L(3,6) = -\sqrt{6}/4$
$Z(4,8) = -\sqrt{6}/24$		
$Z(4,9) = -5\sqrt{6}/24$		
$Z(5,7) = \sqrt{3}/4$		
$Z(5,8) = -\sqrt{2}/4$		
$Z(6,8) = \sqrt{6}/8$		
$Z(6,9) = -\sqrt{6}/24$		
$Z(7,9) = -\sqrt{6}/12$		
$Z(8,9) = -1/4$		
$Z(8,10) = \sqrt{6}/4$		
$Z(9,9) = 1/6$		
$Z(9,10) = -\sqrt{6}/12$		
$Z(10,10) = -1/2$		

A lot of numerical calculation results show that such a set of simplified matrices in (3) is a very good approximation of the set of matrices in (2), the error in the magnetic moment calculated in the spin-transition region is always less than 1%. Therefore the ${}^6A_1-{}^4T_1-{}^2T_2$ coupling model and the simplified matrices can well be applied to study the electronic and magnetic structures of the spin-transition Fe(III) molecules mentioned above.

III. Electronic and Magnetic Structure in the Spin-Transition Region

(i) Qualitative Studies. The ground-state properties of a Fe(III) molecule depend on two opposite physical interactions, i.e., the electron−electron repulsion H_{ee} and the ligand-field H_c. The H_{ee} makes a parallel arrangement of the electronic spins; H_c splits the d orbits and makes an antiparallel arrangement of the electronic spins. When the two interactions are comparable, an electron in the highest suborbital may transfer into the lowest suborbital and changes its spin direction. Therefore the ground state of the Fe(III) molecules can change from high-spin state ${}^6A_1$ into low-spin state ${}^2T_2$ or reversely when increasing or decreasing the crystal-field strength parameter Dq. Such a spin-transition phenomenon can be seen in the well-known Sugano diagram[18] from the crossover of the two energy levels ${}^2T_2$ and ${}^6A_1$. In this case the crossover point is just the spin-transition point and may be called the critical point. Such a spin transition is obviously of a discontinuous type. It should be indicated that the Sugano diagram[18] gives only a rough description of the energy levels, it cannot reflect the fine structures of the levels and the magnetic properties, especially within the spin-transition region, since it is obtained from energy matrices without a spin−orbit coupling mechanism.

When spin−orbit coupling is taken into account, each of ${}^2T_2$ and ${}^6A_1$ will split into two levels E″ and U′, and the spin-transition will occur with out any level crossover, as can

TABLE 5: Components in the Quantum−Admixture Ground State Calculated within the Spin-Transition Region for a Set of Values of ΔDq, Where $\Delta Dq = Dq - Dq_0$ and $Dq_0 = 1637.311$ cm^{-1}, C_6 stands for the components of $^6A_1$, and C_2 stands for the components of $^2T_2$[a]

ΔDq (cm^{-1})	−60	−40	−20	0	20	40	60
C_6	0.9885672	0.9844002	0.9661484	0.4880420	0.0211308	0.0052051	0.0021871
C_2	0.0021539	0.0051456	0.0210014	0.4880413	0.9616079	0.9800188	0.9844192
a (cm^{-1})	1.8677	3.1665	7.2646	57.2286	384.6172	648.3824	655.6670

[a] The calculated values of the zero−field splitting parameter a are also listed below.

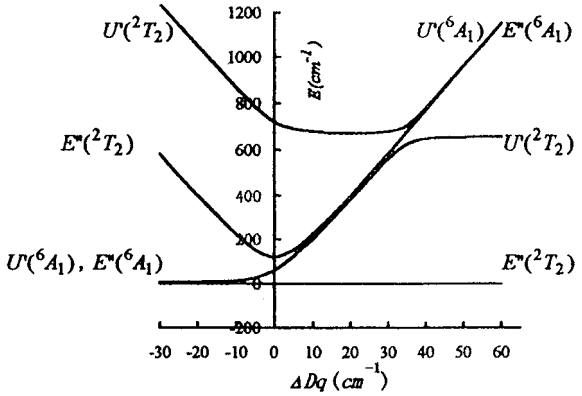

Figure 1. Lowest lying four levels of the Fe(III) ion in the $^6A_1-^2T_2$ spin-transition region.

be seen in our calculation result (Figure 1). When Dq increases (with fixed B, C, and ζ) in this situation, the ground state will change its ratio of components gradually from the case that $^6A_1$ is dominant into the case that $^2T_2$ is dominant. Thus the spin-transition point (critical point) is of course the point at which these two components reach equality. The corresponding value of Dq is called the critical crystal-field strength and denoted as Dq_0. Such a sort of spin transition is of the continuous type.

(ii) Numerical Calculation. In the following calculations, the values of B, C, and ζ are determined according to the Curie method[19] by

$$B = B_0N^4 \qquad C = C_0N^4 \qquad \zeta = \zeta_0N^2 \tag{4}$$

where $B_0 = 1050$, $C_0 = 3806$, and $\zeta_0 = 440$ cm^{-1} are the values for a free Fe(III) ion and N is the average covalence coefficient. The change of N affects strongly the spin-transition point Dq_0 but affects very little the shape of the diagram of the lowest lying levels. Therefore, to get a general understanding for the changing fashion of the lowest lying levels, we need only take for N a typical value, e.g., $N = 0.9$. This value is just suitable for the special molecule that will be studied in section IV. In this case the calculated spin-transition point is $Dq_0 = 1637.311$ cm^{-1}.

The calculated results show that the spin-transition region is around -30 cm$^{-1} < \Delta Dq < 60$ cm^{-1}, where $\Delta Dq = Dq - Dq_0$ and $Dq_0 = 1637.311$ cm^{-1}. The length of the region is close to that obtained by Maltempo et al.[10,11] for the $^6A_1-^4A_1$ spin-transition. Our energy level diagram is shown in Figure 1. The variation of the components in the ground state is shown in Table 5. It can be seen from Table 5 and Figure 1 that at the critical point $\Delta Dq = 0$ the quantum mixture of the ground state is

$$48.8\%\ (^6A_1) + 48.8\%\ (^2T_2) + 2.4\%\ (^4T_1)$$

i.e., the two components of $^6A_1$ and $^2T_2$ are equal to each other, and the gap between the two curves of E″($^6A_1$) and E″($^2T_2$) reaches to the minimum. This is just the criterion of the critical point. The HS−LS transition occurs substantially between E″-($^6A_1$) and E″($^2T_2$). It can also be seen that the splitting between the two curves of the 4-fold degenerated substates U′($^6A_1$) and U′($^2T_2$) reaches the minimum at the point $\Delta Dq \cong 35$ cm^{-1}, which is just the spin-transition point for these two substates.

It should be indicated that though the spin−orbit coupling between $^6A_1$ and $^2T_2$ is realized indirectly through $^4T_1$, but that the mechanism of the HS ↔ LS transition is the mixture of $^2T_2$ and $^6A_1$ instead of $^4T_1$ and $^6A_1$, the latter is very small.

Now let us turn to the study of the magnetic properties.

First, we have obtained the lowest lying six Zeeman levels by diagonalizing the matrices in (3) with various values of H, the results show that some of the levels are flexural and intersect each other. However, when H is small, e.g., $\mu_BH \leqslant 0.1$ cm^{-1}, all the levels are straight. Therefore, we can well calculate the magnetic moments in this region.

To calculate the effective magnetic moment, μ_{eff}, under the weak magnetic field condition, we have used the well-known Van Vleck formula[17]

$$\mu_{eff} = 3kT\{[\sum_i W_1^2(i)/kT - 2W_2(i)]e^{-W_0(i)/kT}\}/\sum_i e^{-W_0(i)/kT} \tag{5}$$

where $W_0(i)$, $W_1(i)$, and $W_2(i)$ are the Zeeman coefficients corresponding to the ith eigenvalue $E(i)$ of our matrices and defined by the Zeeman energy expansion

$$E(i) = W_0(i) + H'W_1(i) + H'^2W_2(i) + ... \tag{6}$$

where $H' = \mu_BH$. Omitting the high-order terms in (6) and taking $H' = 0$, h, and $2h$ ($h = 0.001$ cm^{-1}) in turn and denoting the corresponding $E(i)$ as E_{i0}, E_{i1}, and E_{i2}, respectively, we obtain

$$W_0(i) = E_{i0}$$
$$W_1(i) = [4(E_{i1} - E_{i0}) - (E_{i2} - E_{i0})]/2h$$
$$W_2(i) = [(E_{i2} - E_{i0}) - 2(E_{i1} - E_{i0})]/2h^2 \tag{7}$$

Our analyses shows that the Zeeman coefficients for the lowest lying 12 eigenvalues (they are listed in Table 6) are sufficient for calculating the magnetic moments of a d^5 system in the spin-transition region. The calculated effective magnetic moments for such Fe(III) complex molecules are listed also in Table 6.

It is interesting, as can be seen from our calculated results for various Dq and h, that the first order Zeeman coefficients show some "total symmetry" (i.e., they always have $\sum_{i=1}^{12} W_1(i) = 0$) and that the sum of the second-order Zeeman coefficients is a constant about 0.003.

In the spin-transition region, the temperature dependence of the effective magnetic moment μ_{eff} for a set of values of ΔDq is shown in Figure 3, while the ΔDq dependence of μ_{eff} for a set of values of temperature is shown in Figure 4.

TABLE 6: Zeeman Coefficient $W_j(i)$ and the Effective Magnetic Moment μ_{eff} for Fixed $B_0 = 1050$, $C_0 = 3806$, and $\zeta_0 = 440$ cm^{-1} and a Set of Values of ΔDq, Where $\Delta Dq = Dq - Dq_0$ and $Dq_0 = 1637.311$ cm^{-1} [a]

	ΔDq (cm^{-1}), μ_{eff} (μ_B)						
	−30, 5.8508	−20, 5.7729	−10, 5.6051	0, 5.2663	10, 4.7209	20, 4.0780	30, 3.5461
$W_0(1)$	0.0000	0.0000	0.0000	0.0000	0.0000	0.0000	0.0000
$W_0(2)$	0.0000	0.0000	0.0000	0.0000	0.0000	0.0000	0.0000
$W_0(3)$	4.5187	7.2646	15.0065	57.2286	204.3066	384.6172	562.4875
$W_0(4)$	4.5187	7.2646	15.0065	57.2286	204.3066	384.6172	562.4875
$W_0(5)$	4.5187	7.2646	15.0065	57.2286	204.3066	384.6172	562.4875
$W_0(6)$	4.5187	7.2646	15.0065	57.2286	204.3066	384.6172	562.4875
$W_0(7)$	583.1613	398.8369	224.6391	119.7159	225.2770	399.7247	584.3610
$W_0(8)$	583.1613	398.8369	224.6391	119.7159	225.2770	399.7247	584.3610
$W_0(9)$	1238.4470	1050.8081	868.3109	720.6186	678.5651	672.1752	678.4236
$W_0(10)$	1238.4470	1050.8081	868.3109	720.6186	678.5651	672.1752	678.4236
$W_0(11)$	1238.4470	1050.8081	868.3109	720.6186	678.5651	672.1752	678.4236
$W_0(12)$	1238.4470	1050.8081	868.3109	720.6186	678.5651	672.1752	678.4236
$W_1(1)$	−1.659143	−1.652752	−1.626106	−1.421882	−1.221828	−1.196581	−1.190462
$W_1(2)$	1.659143	1.652753	1.626106	1.421882	1.221828	1.196581	1.190462
$W_1(3)$	−3.658891	−3.657133	−3.654280	−3.648916	−3.636291	−3.591796	−3.176400
$W_1(4)$	−0.998009	−0.997594	−0.996941	−0.995753	−0.993058	−0.983899	−0.901498
$W_1(5)$	0.998009	0.997594	0.996941	0.995753	0.993058	0.983899	0.901498
$W_1(6)$	3.658892	3.657133	3.654280	3.648916	3.636291	3.591796	3.176400
$W_1(7)$	−1.195361	−1.201037	−1.226963	−1.430459	−1.629778	−1.654279	−1.659644
$W_1(8)$	1.195361	1.201037	1.226963	1.430459	1.629778	1.654279	1.659644
$W_1(9)$	−0.280777	−0.280406	−0.280261	−0.280639	−0.282514	−0.290843	−0.407063
$W_1(10)$	−0.071974	−0.070824	−0.068558	−0.063767	−0.051707	−0.007773	−0.372403
$W_1(11)$	0.071974	0.070824	0.068558	0.063768	0.051707	0.007772	0.372402
$W_1(12)$	0.280777	0.280406	0.280261	0.280639	0.282515	0.290843	0.407062
$W_2(1)$	−1.939713	−1.195498	−0.551506	−0.083908	−0.007864	−0.004753	−0.004378
$W_2(2)$	−1.953480	−1.200778	−0.552665	−0.083939	−0.007921	−0.004776	−0.004350
$W_2(3)$	1.953274	1.200280	0.549670	0.015319	−0.373339	−0.548745	−0.345723
$W_2(4)$	0.000033	−0.000015	−0.000060	0.000011	−0.000019	−0.000012	−0.000568
$W_2(5)$	−0.000025	0.000008	−0.000070	−0.000020	−0.000005	−0.000110	−0.000541
$W_2(6)$	1.939526	1.195051	0.548507	0.015248	−0.373804	−0.549872	−0.346122
$W_2(7)$	−0.004085	−0.003810	−0.001306	0.064250	0.377152	0.548653	0.317928
$W_2(8)$	−0.004106	−0.003799	−0.001316	0.064172	0.376586	0.547405	0.317507
$W_2(9)$	−0.000609	−0.000557	−0.000614	−0.000529	−0.000652	−0.000475	0.031740
$W_2(10)$	0.003278	0.003372	0.003329	0.003398	0.003861	0.005192	0.000052
$W_2(11)$	0.003335	0.003367	0.003345	0.003472	0.003769	0.005186	0.000088
$W_2(12)$	−0.000624	−0.000581	−0.000616	−0.000541	−0.000630	−0.000481	0.031771

[a] $W_j(i)$ is calculated by formula 7 with $h = 0.001$ cm^{-1}; μ_{eff} is by formula 5 with T = 300 K.

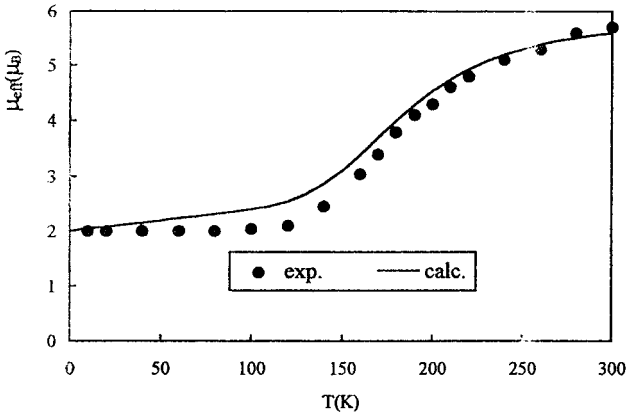

Figure 2. Theoretical curve for the temperature dependence of the magnetic moment μ_{eff} for a Fe(III) ion in a [Fe(3−OEt−SaLAPA)$_2$]-$ClO_4 \cdot C_6H_6$ molecule.

IV. Temperature Dependence of the Magnetic Moment of [Fe(3-OEt-SalAPA)$_2$]$ClO_4 \cdot C_6H_6$ in the Sipn-Transition Region

The variable-temperature experiments reported by Timken et al.[6] show that the [Fe(3−OEt−SalAPA)$_2$]$ClO_4 \cdot C_6H_6$ compound undergoes a gradual but complete spin-crossover transformation (as shown in their Figure 1) and that there are equal populations of high-spin and low-spin complexes at 205 K.

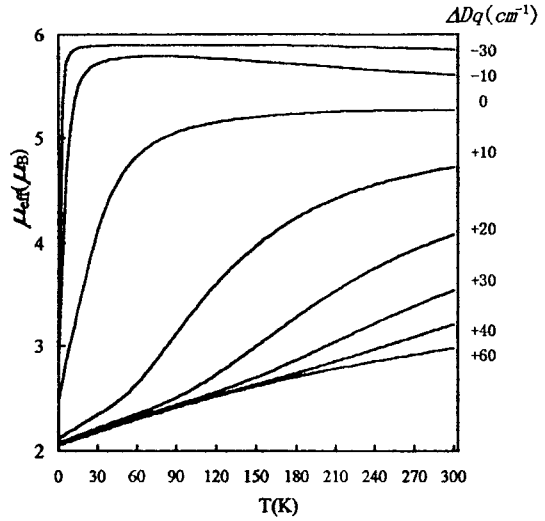

Figure 3. Temperature dependence of the effective magnetic moment μ_{eff} for various ΔDq within the spin-transition region.

As a simulation of the magnetic properties of such a compound with our $^6A_1-^4T_1-^2T_2$ quantum mixture model and according to the bond lengths and bond angles given in ref 6, we may approximately treat the coordination surrounding of the F(III) ion as a cubic symmetry. Then, we may adopt the values of B, C, and ζ used in section II for the Fe(III) molecule,

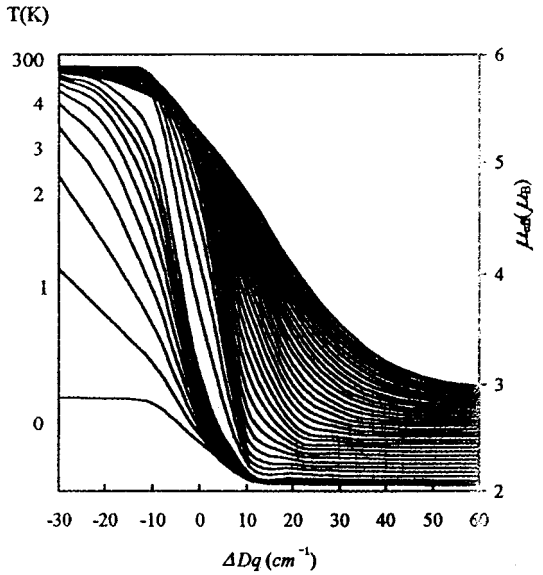

Figure 4. ΔDq dependence of the effective magnetic moment μ_{eff} for various T (K) within the spin-transition region.

thus the HS ↔ LS transition point is still $Dq_0 = 1637.311\ \text{cm}^{-1}$, and the applied magnetic field may be taken along the z-axis. In simulating the thermo-induced spin transition, we considered that the bond lengths of high-spin and low-spin Fe(III) complexes are different from each other. In other words, the coordination surrounding will be changed with temperature. This will definitively lead to a change in Dq. We suggested a nonlinear temperature dependence for Dq as follows:

$$Dq - Dq_0 = 45.9656 - 3.5(T/18) + 0.01(T/18)^2 \quad (8)$$

then, the temperature dependence of the calculated effective magnetic moment is consistent with the experiment curve,[6] as it can be seen in Figure 2. At the spin-transition point, the temperature is just $T = 205$ K and the high-spin and low-spin components are exactly equal, all being 48.804%.

Conclusion

A quantum-admixture model for the description of the HS ↔ LS transition phenomenon of Fe(III) complex molecules has been established on the basis of the UCFC method. By means of this model and the corresponding Hamiltonian matrices, a general study for the dependence of the molecular magnetic moment on the crystal-field strength, within the spin-transition region and for the temperature from 0 to 300 K, has been carried out. A simulation for the temperature dependence of the effective magnetic moment of $[Fe(3-OEt-SalAPA)_2]ClO_4 \cdot C_6H_6$ molecules in the thermo-induced HS ↔ LS transition phenomenon has been carried out. The theoretical results are consistent with the experiments. This shows that our quantum-admixture model is suitable for this case.

Acknowledgment. We wish to thank Prof. Gou Qing-Quan, Chengdu University of Science and Technology, for many helpful discussions. This project was supported by National Natural Science Foundation of China.

References and Notes

(1) Ewald, A. H.; Martin, R. L.; Sinn, E.; White, A. H. *Inorg. Chem.* **1969**, *8*, 1837.
(2) Maeda, Y.; Takashima, Y. *J. Chem. Soc., Dalton Trans.* **1986**, 1115.
(3) Haddad, M. S.; Lynch, M. W.; Federer, W. D.; Hendrickson, D. N. *Inorg. Chem.* **1981**, *20*, 123, 131.
(4) Scheidt, W. R.; Geiger, D. K.; Hages, R. G.; Lang, G. *J. Am. Chem. Soc.* **1983**, *105*, 2625.
(5) Axe, F. U.; Flowers, C.; Loew, G. H.; Waleh, A. *J. Am. Chem. Soc.* **1989**, *111*, 7333.
(6) Timken, M. D.; Strouse, C. E.; Soltis, S. M.; Daverio, S. A.; Hendrickson, D. N.; Abdel-Mawgoud, A. M.; Wilson, S. R. *J. Am. Chem. Soc.* **1986**, *108*, 395.
(7) Federer, W. D.; Hendrickson, D. N. *Inorg. Chem.* **1984**, *23*, 3861.
(8) Petty, R. H.; Dose, E. V.; Tweedle, M. F.; Wilson, L. J. *Inorg. Chem.* **1978**, *17*, 1064.
(9) Hall, G. R.; Hendrickson, D. N. *Inorg. Chem.* **1976**, *15*, 607.
(10) Maltempo, M. M. *J. Chem. Phys.* **1974**, *61*, 2540.
(11) Maltempo, M. M.; Moss, T. H. *Q. Rev. Biophys.* **1976**, *92*, 181.
(12) Harris, G. *Theor. Chim. Acta* **1966**, *5*, 397; **1968**, *10*, 119.
(13) Kuang, X. Y.; Morgenstern-Badarau, I.; Rodriguez, M. C. *Phys. Rev. B* **1993**, *48*, 6676.
(14) Kuang, X. Y.; Morgenstern-Badaratu, I.; Malfant, I. *Phys. Rev. B* **1993**, *47*, 5455. Kuang, X. Y.; Morgenstern-Badarau, I. *Phys. Stat. Sol. b* **1995**, *191*, 395.
(15) Zhou, K. W.; Xie, J. K.; Nimg, Y. M.; Zhao, S. B.; Wu, P. F. *Phys. Rev. B* **1991**, *44*, 7499.
(16) Zhou, K. W.; Yang, J. H.; Peng, L. C. *Chin. Sci. Bull.* **1996**, *41*, 982.
(17) Griffith, J. S. *The Theory of Transition Metal Ions*; Cambridge University Press: Cambridge, U.K. 1961.
(18) Tanabe, Y.; Sugano, S. *J. Phys. Soc. Jpn.* **1954**, *9*, 753.
(19) Curie, D.; Barthou, C.; Canny, B. *J. Chem. Phys.* **1974**, *61*, 3084.